IEEE Access
Multidisciplinary | Rapid Review | Open Access Journal

Received February 22, 2019, accepted March 18, 2019, date of publication March 28, 2019, date of current version April 11, 2019.

Digital Object Identifier 10.1109/ACCESS.2019.2907302

Electrical Tree in HTV Silicone Rubber With Temperature Gradient Under Repetitive Pulse Voltage

TAO HAN[1,2], (Member, IEEE), BOXUE DU[1], (Senior Member, IEEE), TINGTING MA[1], FUYU WANG[1], YU GAO[1], (Member, IEEE), ZHIPENG LEI[2], (Member, IEEE), AND CHUANYANG LI[2], (Member, IEEE)

[1]Key Laboratory of Smart Grid of Education Ministry, School of Electrical and Information Engineering, Tianjin University, Tianjin 300072, China
[2]Department of Electrical Engineering, University of Bologna, 40134 Bologna, Italy

Corresponding author: Yu Gao (hmgaoyu@tju.edu.cn)

This work was supported in part by the Chinese National Natural Science Foundation under Grant 51707132, and in part by the Chinese National Key Research and Development Program under Grant 2018YFB0904400.

ABSTRACT High temperature vulcanized silicone rubber (HTV SIR) is important insulation for high voltage direct current (HVDC) cable accessories. The pulse voltage in the HVDC system may initiate an electrical tree in SIR insulation. During the operation, there is a temperature gradient in SIR caused by the different temperatures of conductor and external environment. So it is necessary to research the electrical tree initiated by pulse voltage under the temperature gradient. In this paper, electrical trees in SIR with different temperature gradients were recorded. The inception voltage, tree length, and accumulated damage (AD) distribution were analyzed. The experiment results indicate that tree inception voltage decreases with the increase of temperature of the ground electrode when the needle temperature is 90 °C, it also decreases with the increase of needle temperature when the ground temperature is 90 °C. All the trees are in bush structure when the ground temperature is 90 °C, the structure changes from branch to bush with the increase of ground temperature when the needle temperature is 90 °C. When the needle temperature is 90 °C, AD distribution changes obviously with the increase of ground temperature. The conductivity of SIR under different temperatures and electric fields was tested. The effect of changing conductivity on tree inception was discussed. Surface potential decay (SPD) at different temperatures was tested. The trap characteristics and charge kinetic properties influenced by temperature may be the main reasons for the change of tree structures in the growth process.

INDEX TERMS Electrical tree, HVDC cable, pulse voltage, silicone rubber, temperature gradient.

I. INTRODUCTION

High voltage direct current (HVDC) cable has been widely researched and operated [1], [2]. In the operation of HVDC cable, the insulation in cable accessories has been proven to be the weakest point [3]–[6]. Composite multilayer insulation is usually employed in the cable accessories [2], [7]–[10]. Space charge and different conductivity of insulations make the distortion of electric field inside cable accessories more severe [11]–[15], easily leading to the insulation degradation.

The associate editor coordinating the review of this manuscript and approving it for publication was Ahmad Elkhateb.

Electrical tree is an electrical degradation can be caused by the distorted electric field [16]–[19]. Different from AC electrical tree, DC electrical tree is difficult to be initiated because of the shielding effect of homo space charges under stable DC voltage [20]–[22]. However, there are impulse voltage in DC system, coming from the overhead line, convertor station and operation [23]–[26]. According to the previous research, the pulse voltage can reduce the tree inception voltage and play an important role in the growth of tree in HVDC cable [27], [28].

In cable accessories, high temperature vulcanized silicone rubber (HTV SIR) is usually used as main insulation in the stress cone [8]. Its operation temperature varies

from −55 to 180 °C. While in the operating condition, the highest temperature occurs near to the conductor and decreases from conductor to outer semi-conductive layer, producing a temperature gradient in the radial direction [29], [30].

Temperature is an important factor influencing the dielectric properties of SIR, especially the conductivity [31], [32]. Temperature gradient will change the electric field distribution under DC and pulse voltage [29], [33], [34]. It was also found that temperature will affect tree structure and its growth characteristics [35]–[37]. However, most of the papers about temperature research the isothermal treeing process. This is different from the real operating condition. It can be speculated that tree would be influenced by the varying temperature in the growth process. Besides, the temperature also changes the mobility of charge carriers. This varying dynamic characteristics may also change the treeing characteristics.

In this paper, electrical trees in HTV SIR samples were investigated under different temperature gradients. The conductivity and surface potential decay (SPD) at different temperatures were tested. Trees under repetitive pulse voltage with different temperature gradients have been initiated. The relationship between tree inception and conductivity was discussed. The treeing process has been recorded and the effects of conductivity and trap distribution on treeing process were discussed. It has been found that with different temperature gradients, tree structure is dependent on the charge accumulation influenced by the varying charge kinetic properties and trap characteristics.

II. EXPERIMENTAL SETUP

A. SAMPLE PREPARATION

HTV SIR (Huayue, HTV 110-2) samples were employed in this experiment. In the preparation process, needle electrodes were inserted into samples before vulcanization. The curvature radius of needle tip was 3 μm. The vulcanization was performed at 175 °C for 10 min under a pressure of 6 MPa. After this, the sample was kept in a thermal tank with 165 °C and 0.1 MPa for 24 h to get a second vulcanization. The HTV SIR sample was cut into small samples for the test, the distance between needle tip and the edge of sample was set to be 2 mm. The dimension of sample was 30 mm × 20 mm with the thickness of 3 mm.

B. EXPERIMENTAL SETUP

The experimental setup was shown in Fig.1. SIR sample was placed on the ground electrode, which was made of a copper plate with the thickness of 1 mm. During the experiment, four heating tapes were employed. Two tapes were attached on the ground electrode. The other two tapes were attached on the both sides of sample, 1 mm beyond the needle tip. Four temperature sensors were attached on the heating tapes for the temperature control. With the heating tapes, different temperature gradients were produced. The high pulse voltage was generated by a transformer which was fed by a low pulse voltage generator. The repetitive frequency of pulse voltage was 200 Hz, the rise and fall time of pulse voltage were 100 and 120 μs, as shown in Fig.2. An HV probe (Tektronix, P6015) and oscilloscope (Tektronix, TBS1000) were used for observing the pulse voltage.

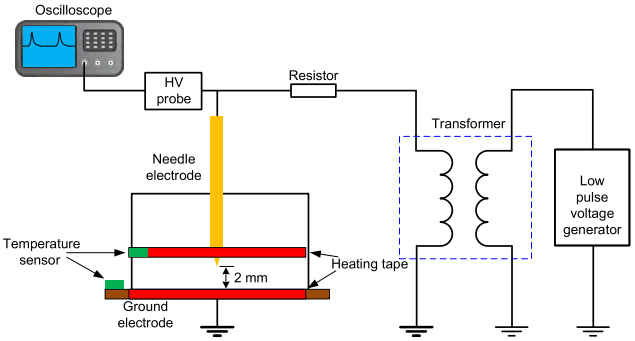

FIGURE 1. Experimental setup for electrical treeing in SIR.

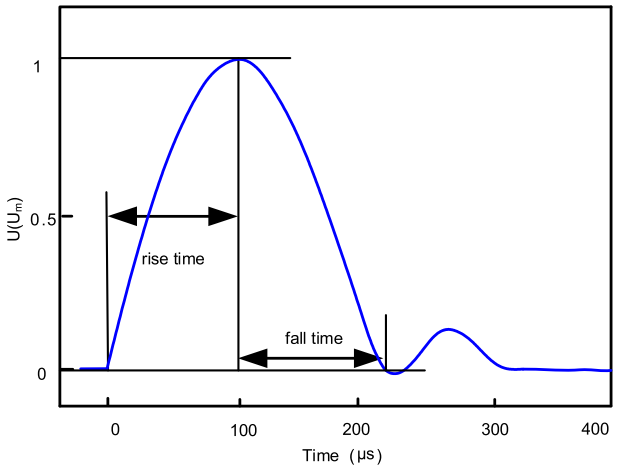

FIGURE 2. Repetitive pulse voltage applied in the experiment.

TABLE 1. Temperature gradient in experiment.

Temperature Gradient	Needle Temperature (°C)	Ground Temperature (°C)
G90N20	20	90
G90N30	30	90
G90N40	40	90
G90N50	50	90
N90G20	90	20
N90G30	90	30
N90G40	90	40
N90G50	90	50

In the tree inception voltage test, the voltage was increased at a rate of 0.2 kV/min until a tree longer than 20 μm was observed. For the treeing growth test, a repetitive pulse voltage with the amplitude of −15 kV was applied onto the needle electrode during the treeing process.

The temperature gradients are shown in TABLE 1, defined to be G90N20 to N90G50. In this work, ''needle temperature'' is used for the temperature of heating tapes near the needle tip, ''ground temperature'' is used for the temperature of heating tapes on ground electrode. The details of temperature

TABLE 2. Parameters used in simulation.

Parameter	Value
Material of needle electrode	Steel
Material of heating tapes	Aluminum oxide ceramic
Material of ground electrode	Copper
Thermal Conductivity of SIR	0.27 W/(m·K)
Thermal Conductivity of air	0.025 W/(m·K)
Thermal Conductivity of needle	45.0 W/(m·K)
Size of SIR sample	30 mm×20 mm×3 mm

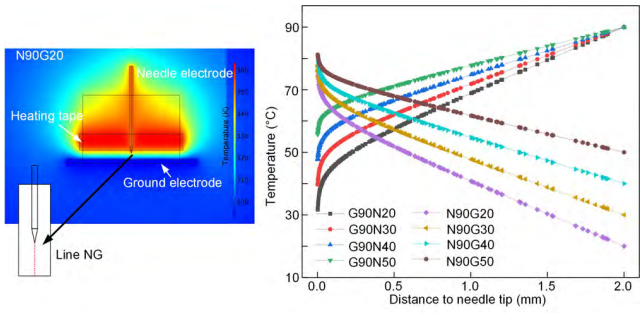

FIGURE 3. Temperature distribution in SIR. (a) Simulation result in SIR 2-D section; (b) Temperature in line NG with different gradients.

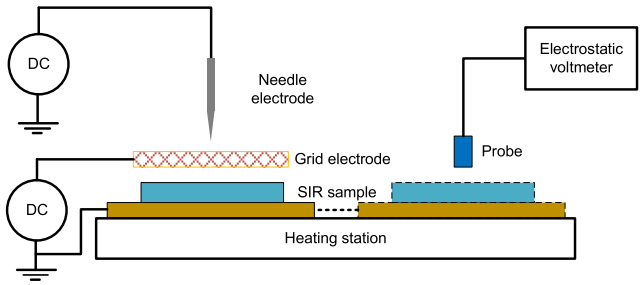

FIGURE 4. Surface potential test setup for SIR.

gradient in SIR were simulated by COMSOL Multiphysics. A 3-D model with the same size of SIR sample was employed in the simulation. The parameters used in simulation is shown in TABLE 2. The temperature in line NG from needle to ground electrode is shown in Fig.3. Before applying the pulse voltage, the temperatures of needle and ground electrodes were kept for 10 min to get the stable gradient.

A digital microscope was employed to record the tree structure at different treeing time. 10 samples were tested under each experimental condition.

C. SPD MEASUREMENT

To calculate the trap distribution in SIR, SPD measurement was employed [38], [39]. As shown in Fig.4, the sample was put on a thermostatic heating plate to control the temperature. Before the test, the surface of sample was charged by negative DC corona. The needle and grid electrodes were employed to control the initial surface potential. The interval between needle electrode and sample surface was 8 mm, while the grid electrode was placed 5 mm above the surface. The voltage applied on the needle electrode was DC of −5 kV. After the

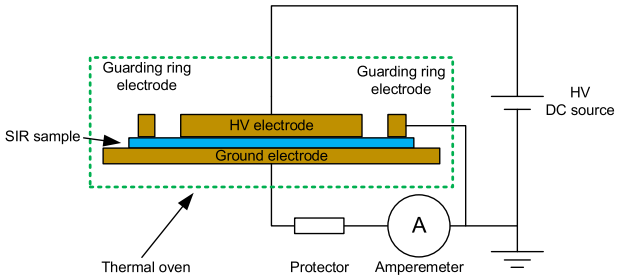

FIGURE 5. Conductivity test setup for SIR.

charging process of 15 min, the sample was moved to the probe of electrostatic voltmeter (Trek 347-3HCE). The probe was positioned 3 mm above the center of sample surface. The decay of surface potential was recorded by this electrostatic voltmeter. The temperature of sample was kept to be 20 to 90°C, the relative humidity was controlled to be 25%.

D. CONDUCTIVITY MEASUREMENT

DC conductivity was tested on a typical three-electrodes system, as shown in Fig.5. The sample and electrodes were put into a thermal oven during the test. The sample for DC conductivity test was in the radius of 1.25 cm and thickness of 300 μm. In this test, the electric field applied onto the sample varied from 1.6×10^6 to 2.7×10^7V/m and temperature changed from 20 to 90°C. The model of ampere meter for the current test was Keithley 6517b. The relative humidity was set to be 25%.

The conductivity was calculated as follows:

$$\sigma = \frac{I}{U} \cdot \frac{l}{\pi r^2} \tag{1}$$

where I is the current in A, U is the applied voltage in V, l is the thickness of sample in m, r is the radius of sample in m. To calculate the precise conductivity, the time of current test was set to be 3 h and the stable current value was picked.

E. ACCUMULATED DAMAGE DISTRIBUTION

With the growth of tree, the width and length change with treeing time. In the research on electrical tree, the accumulated damage (AD) is usually employed to analyze the destroyed area caused by tree, which is usually calculated by summing the pixel number in tree area [40]. However, AD is not precise to distinguish the change of damage in different tree area. To solve this problem, the pixels in different distance from needle tip is calculated in this paper, defined as AD distribution. The calculation procedures are shown in Fig.6.

Fig.6(a) shows the picture of tree at N90G50. To calculate the AD distribution, a picture of 400 × 400 pixels was picked out. The tree area was restructured to be black and white, as shown in Fig. 6(b). The tree area is shown in white color. d is the distance from needle tip in the direction shown in Fig.6(b). With the change of d, pixel numbers of white area in line(d) is added up and the pixel number is defined to be the AD of line(d).

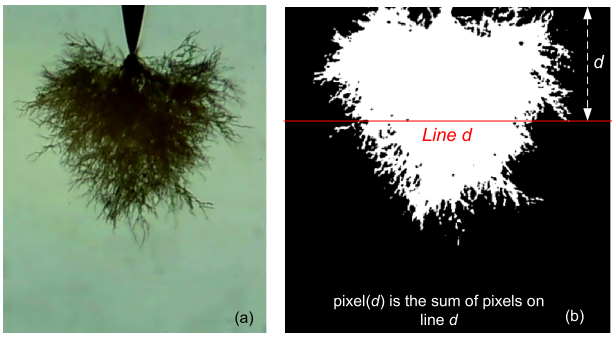

FIGURE 6. Accumulated damage calculation method. (a) tree to be calculated, (b) restructured tree in black and white picture.

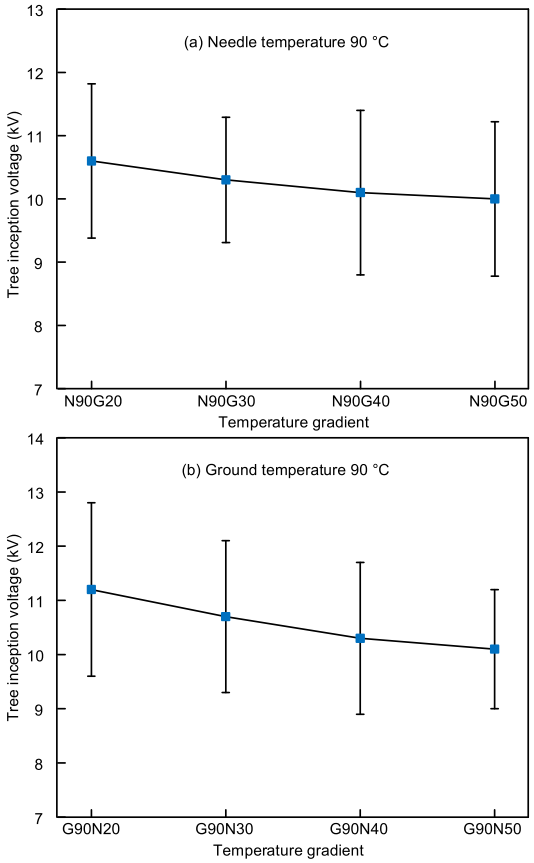

FIGURE 7. Tree inception voltages under different temperature gradients.

III. EXPERIMENT RESULTS

A. EFFECT OF TEMPERATURE GRADIENT ON TREE INCEPTION VOLTAGE

Under each temperature gradient, tree inception voltages of 10 samples were tested. The results are shown in Fig.7. Inception voltage of electrical tree changes with temperature gradient. When the needle temperature is 90°C, the mean value of inception voltage decreases from 10.6 to 10.0 kV with the increase of ground temperature. While with the ground temperature of 90°C, it decreases from 11.2 to 10.1 kV. The difference of inception voltage with needle temperature of 90°C is 0.6 kV and it is 1.1 kV with ground temperature of 90°C.

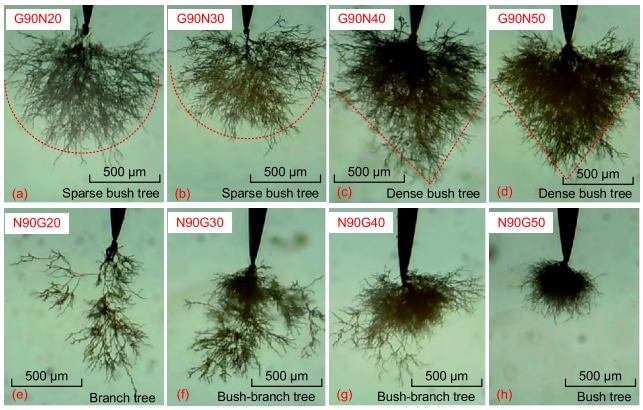

FIGURE 8. Tree structure in 120 min with different temperature gradients.

B. EFFECT OF TEMPERATURE GRADIENT ON TREE STRUCTURE

Under different temperature gradients, different tree structures have been found. As shown in Fig.8(a) to (d), when the ground temperature is fixed to be 90°C, the tree structure changes from sparse bush tree to dense bush tree with the needle temperature increasing from 20 to 50°C. The outlines of these trees change from arc to triangle, which is shown with red line in Fig.8 (a) to (d).

As shown in Fig.8(e) to (h), when the needle temperature is set to be 90°C, the main tree structure at N90G20 is branch tree and it changes to be bush-branch tree when the ground temperature is 30 and 40°C; when the ground temperature is 50°C, the tree structure is typical dense bush tree.

C. EFFECT OF TEMPERATURE GRADIENT ON TREE LENGTH

Tree length is defined as the distance from needle tip to the longest branch tip. After the treeing time of 120 min, the tree length was measured and shown in Fig.9. Tree length with needle temperature of 90°C is shown in Fig.9(a). With the increase of ground temperature, tree length decreases from 1.1 mm to 0.42 mm, with the tree structure changing from branch tree to bush tree as shown in Fig.8.

Fig.9(b) shows the tree length with different needle temperatures when the ground temperature is 90°C. It can be found all the trees are in similar length under different gradients, whose value is around 1 mm.

D. EFFECT OF TEMPERATURE GRADIENT ON AD DISTRIBUTION

AD distribution of tree under each temperature gradient with the needle temperature of 90°C is shown in Fig.10. The blue area is corresponding to the AD at different distance to needle tip in tree area, which is calculated with the method shown in Fig.6. In Fig.10(a), pixel number at each distance is lower than 100, which means that the damage area of branch tree is low in the whole tree area. However, branch tree is a much bigger threat than bush tree to the cable insulation, because it often has a faster growth rate than bush tree. When it

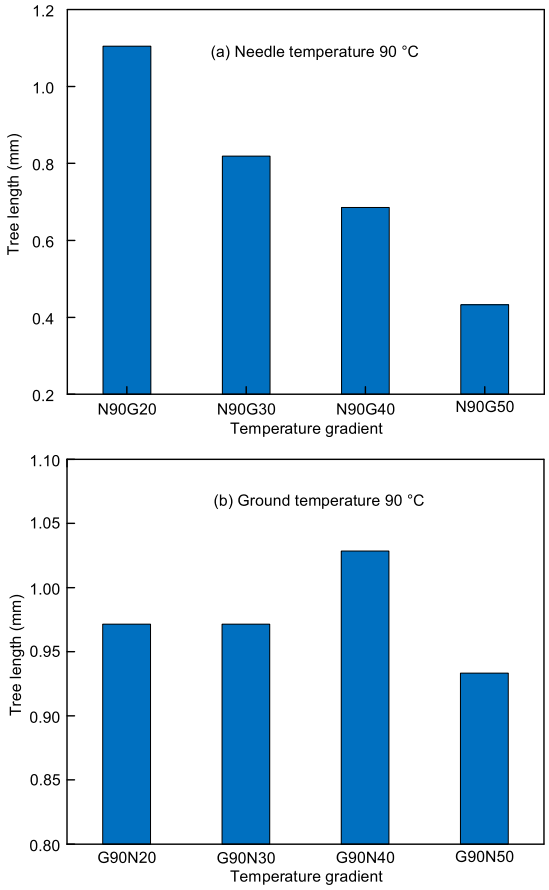

FIGURE 9. Tree length at 120 min with different temperature gradients. (a) tree length with needle temperature of 90°C, (b) tree length with ground temperature of 90°C.

bridges the insulation between the conductor and ground, a breakdown may occur. In Fig.10(b) and (c), pixel number close to needle tip is much higher than branch tree, which is higher than 150. It indicates the appearance of bush area near needle tip. With the increase of distance, pixel number decreases to be lower than 100, which is consistent with the appearance of branch area from the border of bush area. The AD distribution is simpler in Fig.10(d), which is caused by the uniform bush structure. There is a fast increase rate of AD distribution near the needle tip and it decreases sharply on the end of bush area.

Fig.11 shows the AD distribution with the ground temperature of 90°C. In Fig.11(a) and (b), the increase rate of AD distribution is much slower than that in Fig.11 (c) and (d). This is caused by the low channel density in these trees. With the increase of channel density, shapes of AD distribution in Fig.11(c) and (d) are similar to each other. AD increases rapidly to a maximum value of 250-300 pixels. It can be found that the position of maximum AD changes from 0.5 to 0.2 mm with the increase of needle temperature, which indicates that the biggest damage area gets nearer to the needle tip. This is consistent with the change of bush tree outlines shown in Fig.8.

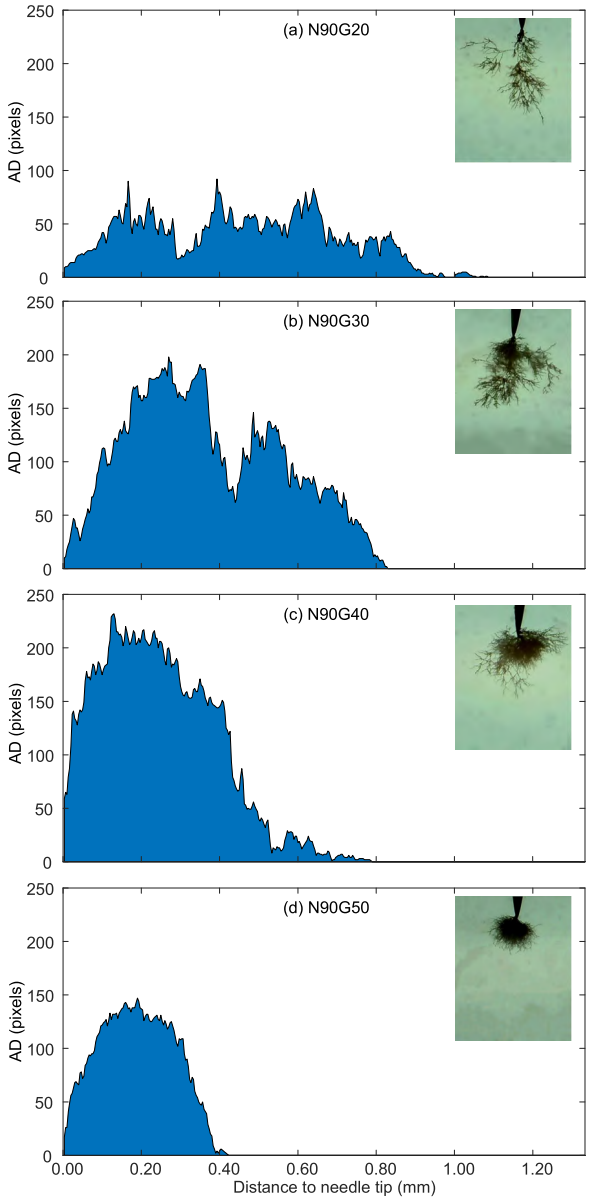

FIGURE 10. AD distribution in trees under gradients with needle temperature of 90°C.

IV. DISCUSSION

A. CONDUCTIVITY OF SIR UNDER DIFFERENT TEMPERATURE AND ELECTRIC FIELD

The effects of temperature and electric field on conductivity have been reviewed by Boggs *et al.* [41]. It shows that conductivity in polymer insulation is dependent on both temperature and electric field.

According to the hopping model of conduction in polymers, the conductivity of SIR can be defined as this formula

$$\sigma(E,T) = A\exp(\frac{-\varphi q}{kBT})\frac{\sinh(B|E|)}{|E|} \quad (2)$$

where $\sigma(E,T)$ is conductivity of SIR; A and B are constant values; q is the elementary charge, 1.6×10^{-19}C; T is

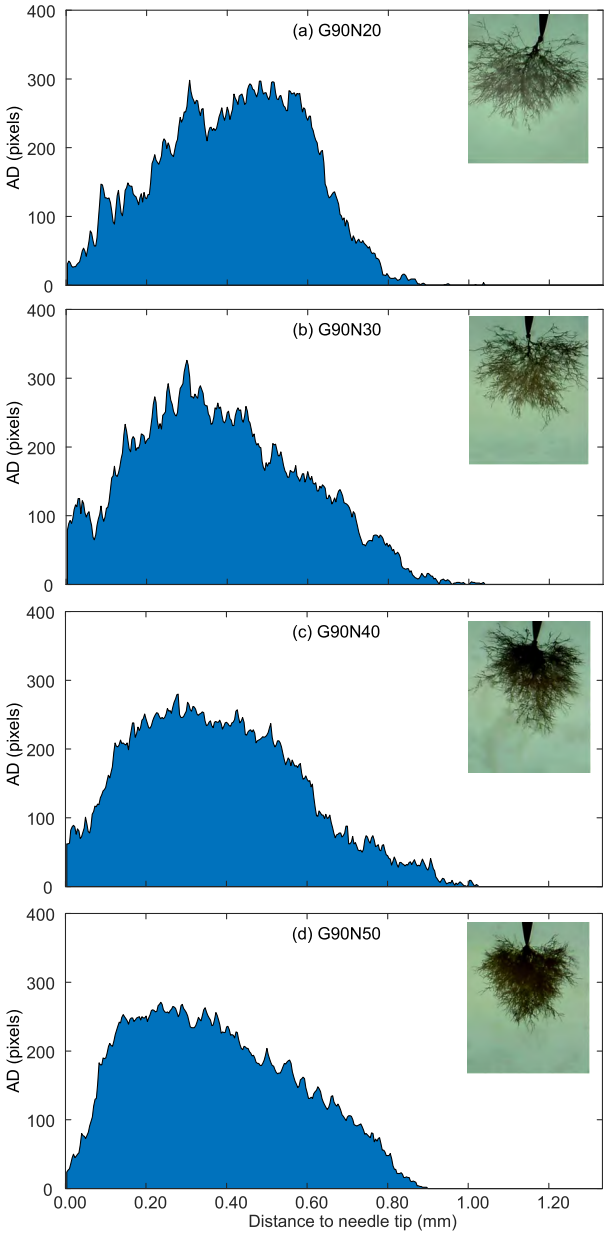

FIGURE 11. AD distribution in trees under gradients with ground temperature of 90°C.

temperature in K; E is the electric field in V/m; φ is thermal activation energy in eV, which can be roughly calculated from the conductivity at different temperature according to the formula

$$\sigma = \frac{N}{T}\exp(\frac{-\varphi}{k_B T}) \tag{3}$$

where N is constant.

The tested conductivity at different temperature with electric field of 6.67×10^6V/m is employed to calculate the activation energy. According to (3), the $\ln(\sigma T)$ is linear to $1/T$, the slope of fitting line in Fig.12 is -4.08, which is $-\varphi/k_{\mathrm{B}}$. The activation energy for SIR is 0.35 eV.

According to [41], the fitting process for (2) is as follows. The current density at 303.15 K was tested and shown in

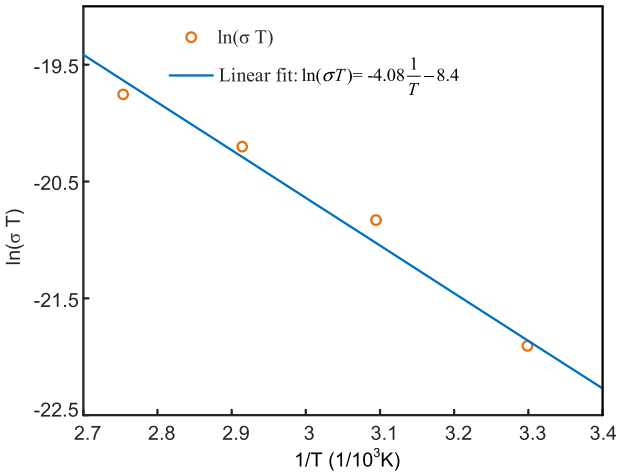

FIGURE 12. ln(σT) versus 1/T and its linear fitting.

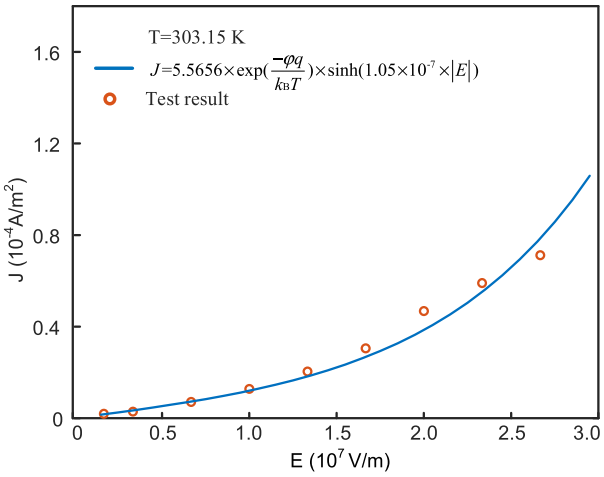

FIGURE 13. Current density(J) under different electric field (E) at 303.15 K and its curve fitting.

Fig.13. The electric field was set to be 1.67×10^6 ~2.67×10^7 V/m. The curve of electric field and current density was fit to

$$J(E)|_T = \mathrm{C} \cdot \sinh(\mathrm{D} \cdot |E|) \ldots\ldots \tag{4}$$

where C and D are constants.

The current density at temperature from 303.15 to 363.15 K was tested and shown in Fig.14, with the electric field of 6.67×10^6 V/m. The curve of temperature and current density was fit to

$$J(T)|_E = \mathrm{F} \cdot \exp(\frac{-\varphi q}{k\mathrm{B}T}) \tag{5}$$

where F is constant.

Then the current density can be written in

$$J(E,T) = A\exp(\frac{-\varphi q}{kBT})\sinh(B|E|) \tag{6}$$

where $\mathrm{A} = 5.5656$, $\mathrm{B} = 1.05 \times 10^{-7}$. According to

$$J(E,T) = \sigma(E,T) \cdot |E| \tag{7}$$

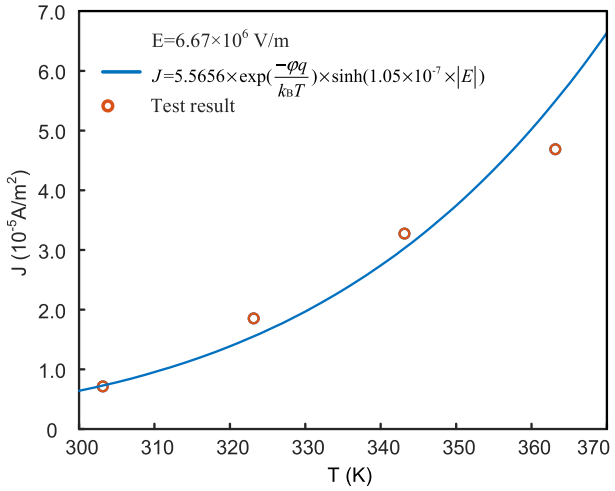

FIGURE 14. Current density(J) at different temperature (T) under 6.67 × 10^6 V/m and its curve fitting.

The equation for conductivity of SIR employed in this work can be written in

$$\sigma(E,T)=5.5656\times\exp(\frac{-\varphi q}{kBT})\frac{\sinh(1.05\times10^{-7}\times|E|)}{|E|} \quad (8)$$

B. TREE INCEPTION UNDER TEMPERATURE GRADIENT

As discussed in our previous research [28], tree inception under pulse voltage is different from that under AC.

Without considering the shielding effect of homo space charges, the maximum electric field can be calculated by Mason equation:

$$E_{\max}=\frac{2U}{r\ln(1+4d/r)} \quad (9)$$

where U is the amplitude of applied voltage in V, r is the curve radius in m, d is the distance between needle tip and ground electrode in m.

After the application of repetitive pulse voltage, space charges will be injected into SIR following the Schottky-Richardson injection [42]. With the shielding effect of injected space charges, electric field near the needle tip will be decreased to be much lower in about 20-50 μm [22], [43]–[46], [48]. We can roughly assume the area within 50 μm from needle tip to be the space charge region. When the needle temperature is 90°C, the temperature of area near the needle tip is around 80 °C as shown in Fig.3. With the ground temperature changing from 20 to 50°C, the temperature at 50 μm varies from 66.55 to 76.00°C. This will increase the conductivity of SIR near the needle tip. While with the increase of pulse voltage, electric field caused by the pulse voltage will keep increasing. According to (8), the conductivity around needle tip will be higher with the pulse voltage [49]. During the interval of two pulses, the change of electric field is similar to the situation in inception of grounded DC tree. At this time, the transformer coil is still connected to the needle electrode through a resistor. Without the input of low pulse voltage, there is no high voltage in this coil, as shown in Fig. 1. Because the space charges were injected into SIR by the previous pulses, there will be an electric field near the needle tip produced by these space charges. If this field strength is higher than the material dielectric strength, a partial breakdown will occur and a tree channel will be generated. Meanwhile, some space charges will escape from the traps and migrate towards the needle tip, weakening this local electric field caused by these injected space charges [40], [50]. This migration will stop after the electric field decreases to a fixed value, as discussed in [28]. When the next pulse is applied, new charges will be injected into SIR and the migration of charges will be repeated. In this process, the molecular chains of SIR may be broken by the partial breakdown or collision with hot electrons, leaving a crack with gaseous product near the tip. Besides, the current in this area will produce Joule heat and enlarge the crack near needle tip. These may be the dominant reason for tree inception under repetitive pulse voltage. With the higher temperature of area near needle tip, the higher conductivity of SIR in this area will contribute to the charge injection and migration. The result in Fig.7(a) shows that the mean value of tree inception voltage is decreased slightly with the increase of ground temperature. This change is maybe caused by the different conductivity and charge migration process.

It can be found that under temperature gradients from G90N20 to G90N50, the temperature on border of space charge region increases from 42.03 to 61.98°C. It indicates that the conductivity here increases and Joule heat produced by migration of space charge will be much higher with the increasing needle temperature. Besides, the molecular kinetic energy of SIR is increased by higher temperature. With this intense molecular thermal motion, the chemical bond in molecular will be easier to be broken by the collision with space charge. This will lead to the lower tree inception voltage with higher needle temperature.

C. TREE GROWTH UNDER TEMPERATURE GRADIENT

After the initiation of tree, there will be a fast growth stage lasting for several minutes, then different tree structures will be formed in the treeing process. With the growth of tree, the electric field and temperature around the channel tube will be changed because of the temperature gradients.

During the growth of tree, partial discharge inside the tube is one of the main accelerating factors [27], [51]. The partial discharge in tree channels can be caused by accumulation of space charge in the tube. As is known, the trap distribution and charge kinetic energy are important factors in this accumulation process. They will influence the charge migration through SIR bulk [52]. With temperature gradient, trap characteristics and migration of space charges will be different and influence the tree growth.

To analyze these factors, SPD test was carried out. The normalized SPD results of 30 to 90°C shown in Fig.15 manifest that the surface potential decays faster with the increase of temperature. The SPD test at 20, 40, 60 and 80°C are also

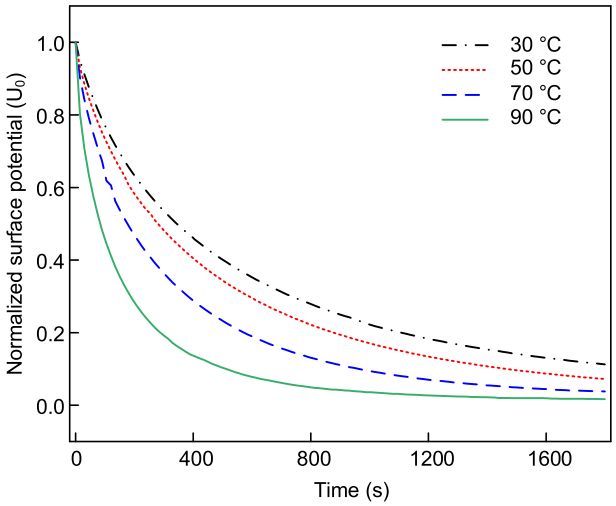

FIGURE 15. SPD test results of SIR under different temperatures.

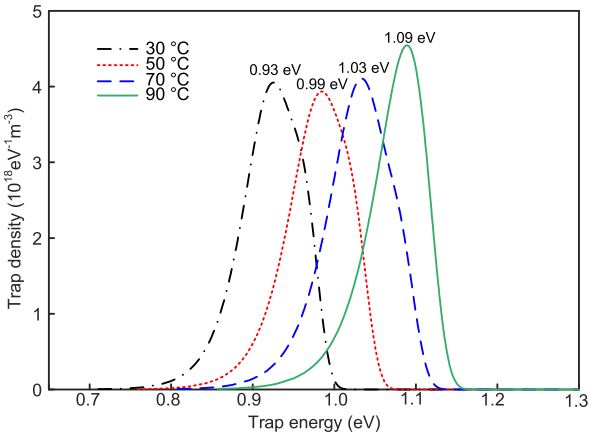

FIGURE 16. Trap distribution at different temperature.

in the same tendency. It indicates that the charges escape faster through SIR bulk to the ground with the increase of temperature.

The SPD equation is developed from the isothermal time-dependent current theory proposed by Simmon and Tams [53]. The trap distribution is calculated based on the detrapping process, which is relative to the carriers escaping from traps. According to this theory, these trap energy and density can be calculated by the two equations

$$E_{\mathrm{T}} = k_{\mathrm{B}} T \ln(v_{\mathrm{ATE}} t) \tag{10}$$

$$N\mathrm{T} = \frac{4\varepsilon_0 \varepsilon_r}{q k_{\mathrm{B}} T L^2} \left| t \frac{dU_s}{dt} \right| \tag{11}$$

where E_{T} is the trap energy in eV, k_{B} is the Boltzmann's constant, T is the temperature in K, v_{ATE} is the attempt to escape frequency in s^{-1}, N_{T} is the trap density in $\mathrm{eV}^{-1}\mathrm{m}^{-3}$, ε_0 and ε_{r} are the permittivity of vacuum and the relative permittivity of SIR, q is the elementary charge in C, L is the sample thickness in m, U_{s} is the surface potential in V, t is the decay time in s.

The calculation results are shown in Fig.16. It should be noted that v_{ATE} Can be expressed by the equation

$$v_{\mathrm{ATE}} = \frac{k_{\mathrm{B}} T}{h} \tag{12}$$

where h is the Planck constant in J·s. It indicates that the attempt to escape frequency increases with temperature linearly. With the higher temperature, the charges will get a higher kinetic energy because of the thermal motion. In this motion, the charges will get more chances to escape from the deep traps.

With the increase of temperature, there is a higher energy level of the traps where the charges escape from, the peak value increases from 0.93 to 1.09 eV. It means more and more charges escape from the traps with higher energy level [31], [54]–[56].

In the growth of electrical tree, the tip of tree channel will get closer to the ground electrode. With the needle temperature of 90°C, temperature in the same distance from needle tip will be lower with the decrease of ground temperature. With the lower temperature, more charges will be captured by deep traps around the tree channels, producing a higher local electric field. A partial discharge with higher intensity may be caused by this electric field and a long branch channel may be generated. With lower temperature, this long branch channel will grow towards ground in a branch structure. Even in the growth of bush tree, a branch area will also be generated with the decrease of temperature. As shown in Fig.8(f) and (g), there is a branch area generated from the border of bush area. It is because v_{ATE} decreases and more space charges are captured on the border of bush area with the lapse of time.

As shown in Fig.8(a) to (d), sparse bush tree changes to be dense bush from 20 to 50°C when the ground temperature is 90 °C. This is also caused by the change of charge mobility. When the needle temperature is 20 and 30°C, more space charges are trapped around the existing main branches and form a higher electric field. The discharge caused by this electric field will generate long channels from the main branches. With the treeing time of 120 min, a tree with sparse long channels will be formed. With the needle temperature of 40 and 50°C, more charges escape from the traps because of the higher kinetic energies. The electric field produced by the trapped space charges is lower, leading to a partial discharge with lower intensity. A lot of short tiny branches are produced, forming the dense bush area. With the growth of tree length, the temperature of tree tip is higher and more charges will escape from traps. Besides, the electric field will become homogeneous because of the uniform border of tree area. There will be less partial discharge to accelerate the tree growth. As a result, All the bush trees are limited to be about 1 mm long within 120 min.

V. CONCLUSION

Experiments were carried out to research the effect of temperature gradient on treeing in HTV SIR under repetitive pulse voltage. The tree inception and growth were recorded. The effects of changing temperature and electric field on the

treeing process were discussed. The main conclusions are as follows.

1) All the trees are bush structure with different channel densities when the ground temperature is 90°C and all the length is about 1 mm. When the needle temperature is 90°C, tree structure changes from branch to bush with the increase of ground temperature and tree length decreases from 1.1 to 0.4 mm.

2) The AD distribution can describe the change of damage area at different tree length precisely. With the needle temperature of 90°C, AD distribution changes obviously with changing ground temperature, which is caused by the different tree structure. When the ground temperature is 90°C, the peak value of AD distribution shifts towards the needle tip with the increasing needle temperature, which is consistent with the tree outline.

3) During the inception process, the changing conductivity influenced by temperature and electric field is the main reason for the different tree inception voltages. While in the growth process, trap characteristics and charge mobility influenced by temperature gradient may be the main reasons for the change of tree structures.

REFERENCES

[1] R. D. Roservear, "Power cables in 21st century energy development," *IEEE Power Eng. Rev.*, vol. 20, no. 9, pp. 8–10, Sep. 2000.

[2] H. Ghorbani, M. Jeroense, C. O. Olsson, and M. Saltzer, "HVDC cable systems—Highlighting extruded technology," *IEEE Trans. Power Del.*, vol. 29, no. 1, pp. 414–421, Feb. 2014.

[3] H. Ghorbani, A. Abbasi, M. Jeroense, A. Gustafsson, and M. Saltzer, "Electrical characterization of extruded DC cable insulation—The challenge of scaling," *IEEE Trans. Dielectr. Electr. Insul.*, vol. 24, no. 3, pp. 1465–1475, Jun. 2017.

[4] M. Marzinotto and G. Mazzanti, "The statistical enlargement law for HVDC cable lines part 2: Application to the enlargement over cable radius," *IEEE Trans. Dielectr. Electr. Insul.*, vol. 22, no. 1, pp. 202–210, Feb. 2015.

[5] Y. Zhou, S. Peng, J. Hu, and J. He, "Polymeric insulation materials for HVDC cables: Development, challenges and future perspective," *IEEE Trans. Dielectr. Electr. Insul.*, vol. 24, no. 3, pp. 1308–1318, Jun. 2017.

[6] M. S. Khalil, "International research and development trends and problems of HVDC cables with polymeric insulation," *IEEE Elect. Insul. Mag.*, vol. 13, no. 6, pp. 35–47, Nov. 1997.

[7] J. Li, B. X. Du, and H. Xu, "Suppressing interface charge between LDPE and EPDM for HVDC cable accessory insulation," *IEEE Trans. Dielectr. Electr. Insul.*, vol. 24, no. 3, pp. 1331–1339, Jun. 2017.

[8] B. X. Du, Z. L. Li, and J. Li, "Effects of direct fluorination on space charge accumulation in HTV silicone rubber," *IEEE Trans. Dielectr. Electr. Insul.*, vol. 24, no. 3, pp. 2353–2360, Aug. 2016.

[9] B. X. Du, J. Li, and Y. Sekii, "Effects of ZnO particles on space charge of EVA copolymer for HVDC cable accessory insulation," *IEEE Trans. Dielectr. Electr. Insul.*, vol. 24, no. 3, pp. 1503–1510, Jun. 2017.

[10] S. Delpino *et al.*, "Polymeric HVDC cable design and space charge accumulation. Part 2: Insulation interfaces," *IEEE Electr. Insul. Mag.*, vol. 24, no. 1, pp. 14–24, Jan./Feb. 2008.

[11] G. Mazzanti *et al.*, "A protocol for space charge measurements in full-size HVDC extruded cables," *IEEE Trans. Dielectr. Electr. Insul.*, vol. 22, no. 1, pp. 21–34, Feb. 2015.

[12] K. Wu, Y. Wang, X. Wang, M. Fu, and S. Hou, "Effect of space charge in the aging law of cross-linked polyethylene materials for high voltage DC cables," *IEEE Electr. Insul. Mag.*, vol. 33, no. 4, pp. 53–59, Jul. 2017.

[13] Y. Li, M. Tian, Z. Lei, and J. Zhang, "Effect of nano-silica on dielectric properties and space charge behavior of epoxy resin under temperature gradient," *J Phys. D, Appl. Phys.*, vol. 51, no. 12, Mar. 2018, Art. no. 125309.

[14] C. Li, J. Hu, C. Lin, B. Zhang, G. Zhang, and J. He, "Surface charge migration and DC surface flashover of surface-modified epoxy-based insulators," *J Phys. D, Appl. Phys.*, vol. 50, no. 6, Mar. 2017, Art. no. 065301.

[15] C. Y. Li *et al.*, "Understanding surface charge accumulation and surface flashover on spacers in compressed gas insulation," *IEEE Trans. Dielectr. Electr. Insul.*, vol. 25, no. 4, pp. 1152–1166, Aug. 2018.

[16] M. G. Danikas and T. Tanaka, "Nanocomposites—A review of electrical treeing and breakdown," *IEEE Electr. Insul. Mag.*, vol. 25, no. 4, pp. 19–25, Jul./Aug. 2009.

[17] L. A. Dissado, "Understanding electrical trees in solids: From experiment to theory," *IEEE Trans. Dielectr. Electr. Insul.*, vol. 9, no. 4, pp. 483–497, Aug. 2002.

[18] X. Chen, A. R. Mantsch, L. Hu, S. M. Gubanski, J. Blennow, and C.-O. Olsson, "Electrical treeing behavior of DC and thermally aged polyethylenes utilizing wire-plane electrode geometries," *IEEE Trans. Dielectrics Electr. Insul.*, vol. 21, no. 1, pp. 45–52, Feb. 2014.

[19] X. R. Chen, Y. Xu, X. L. Cao, and S. M. Gubanski, "On the conducting and non-conducting electrical trees in XLPE cable insulation specimens," *IEEE Trans. Dielectr. Electr. Insul.*, vol. 23, no. 1, pp. 95–103, Feb. 2016.

[20] H. Kawamura and M. Nawata, "DC electrical treeing phenomena and space charge," *IEEE Trans. Dielectr. Electr. Insul.*, vol. 5, no. 5, pp. 741–747, Oct. 1998.

[21] X. Chen *et al.*, "AC and DC pre-stressed electrical trees in LDPE and its aluminum oxide nanocomposites," *IEEE Trans. Dielectr. Electr. Insul.*, vol. 23, no. 3, pp. 1506–1514, Jun. 2016.

[22] I. Iddrissu, H. Zheng, and S. M. Rowland, "DC electrical tree growth in epoxy resin and the influence of the size of inceptive AC trees," *IEEE Trans. Dielectr. Electr. Insul.*, vol. 24, no. 3, pp. 1965–1972, Jun. 2017.

[23] W. X. Lu and B.-T. Ooi, "DC overvoltage control during loss of converter in multiterminal voltage-source converter-based HVDC (M-VSC-HVDC)," *IEEE Trans. Dielectr. Electr. Insul.*, vol. 18, no. 3, pp. 915–920, Jun. 2017.

[24] C. H. Zhou and P. Wang, "A study of temporary overvoltage at HVDC rectifier stations," in *Proc. IEEE Electr. Power Energy Conf.*, Winnipeg, MB, Canada, Oct. 2011, pp. 211–215.

[25] N. G. Hingorani, "Transient overvoltage on a bipolar HVDC overhead line caused by DC line faults," *IEEE Trans. Power App. Syst.*, vol. PAS-89, no. 4, pp. 592–610, Apr. 1970.

[26] H. Liu, Y. Li, Y. Liu, M. Zhang, X. Xu, and A. Liu, "Electrical tree initiation properties in cross-linked polyethylene under DC-Impulse composite voltages," *IEEE Access*, vol. 6, pp. 62890–62897, Nov. 2018.

[27] B. X. Du, T. Han, and J. G. Su, "Electrical tree characteristics in silicone rubber under repetitive pulse voltage," *IEEE Trans. Dielectr. Electr. Insul.*, vol. 22, no. 2, pp. 720–727, Apr. 2017.

[28] T. Han, B. X. Du, and J. G. Su, "Electrical tree initiation and growth in silicone rubber under combined DC-Pulse voltage," *Energies*, vol. 11, no. 4, p. 764, Feb. 2017.

[29] W. Choo, G. Chen, and S. G. Swingler, "Electric field in polymeric cable due to space charge accumulation under DC and temperature gradient," *IEEE Trans. Dielectr. Electr. Insul.*, vol. 18, no. 2, pp. 596–606, Apr. 2011.

[30] D. He, W. Wang, J. Lu, G. Teyssedre, and C. Laurent, "Space charge characteristics of power cables under AC stress and temperature gradients," *IEEE Trans. Dielectr. Electr. Insul.*, vol. 23, no. 4, pp. 2404–2412, Aug. 2016.

[31] B. X. Du, Z. R. Yang, Z. L. Li, and J. Li, "Temperature-dependent nonlinear conductivity and carrier mobility of silicone rubber/SiC composites," *IEEE Trans. Dielectr. Electr. Insul.*, vol. 25, no. 3, pp. 1080–1087, Jun. 2008.

[32] W. Song *et al.*, "Aging characterization of high temperature vulcanized silicone rubber housing material used for outdoor insulation," *IEEE Trans. Dielectr. Electr. Insul.*, vol. 22, no. 2, pp. 961–969, Apr. 2015.

[33] X. Chen, X. Wang, K. Wu, Z. R. Peng, Y. H. Cheng, and D. M. Tu, "Space charge measurement in LPDE films under temperature gradient and DC stress," *IEEE Trans. Dielectr. Electr. Insul.*, vol. 17, no. 6, pp. 1796–1805, Dec. 2010.

[34] Z. Lei *et al.*, "Influence of temperature on dielectric properties of EPR and partial discharge behavior of spherical cavity in EPR insulation," *IEEE Trans. Dielectr. Electr. Insul.*, vol. 22, no. 6, pp. 3488–3497, Dec. 2015.

[35] X. R. Chen, Y. Xu, X. Cao, and S. M. Gubanski, "Electrical treeing behavior at high temperature in XLPE cable insulation samples," *IEEE Trans. Dielectr. Electr. Insul.*, vol. 22, no. 5, pp. 2841–2851, Oct. 2015.

[36] T. Han, B. X. Du, Y. Yu, and X. Q. Zhang, "Effect of cryogenic temperature on tree characteristics in silicone rubber/SiO_2 nanocomposites under repetitive pulse voltage," *IEEE Trans. Appl. Supercond.*, vol. 26, no. 7, Oct. 2016, Art. no. 0501404.

[37] B. X. Du, Z. L. Ma, Y. Gao, and T. Han, "Effect of ambient temperature on electrical treeing characteristics in silicone rubber," *IEEE Trans. Appl. Supercond.*, vol. 18, no. 2, pp. 401–407, Apr. 2011.

[38] A. T. Hoang, Y. V. Serdyuk, and S. M. Gubanski, "Mechanisms of surface potential decay on enamel wire coatings," *IEEE Trans. Dielectr. Electr. Insul.*, vol. 22, no. 6, pp. 3470–3480, Dec. 2015.

[39] S. Alam, Y. V. Serdyuk, and S. M. Gubanski, "Potential decay on silicone rubber surfaces affected by bulk and surface conductivities," *IEEE Trans. Dielectr. Electr. Insul.*, vol. 22, no. 2, pp. 970–978, Apr. 2015.

[40] Y. Wang, F. Guo, J. Wu, and Y. Yin, "Effect of DC prestressing on periodic grounded DC tree in cross-linked polyethylene at different temperatures," *IEEE Access*, vol. 18, pp. 25876–25884, Nov. 2017.

[41] S. Boggs, D. H. Damon, J. Hjerrild, J. T. Holboll, and M. Henriksen, "Effect of insulation properties on the field grading of solid dielectric DC cable," *IEEE Trans. Power Del.*, vol. 16, no. 4, pp. 456–461, Oct. 2001.

[42] L. A. Dissado and J. C. Fothergill, *Electrical Degradation and Breakdown in Polymers*. London, U.K.: Peter Peregrinus, 1992.

[43] R. W. Hare, R. M. Hill, and C. J. Budd, "Modelling charge injection and motion in solid dielectrics under high electric field," *J Phys. D, Appl. Phys.*, vol. 26, no. 7, pp. 1084–1093, Mar. 1993.

[44] C. Jörgens and M. Clemens, "Modeling the electric field in polymeric insulation including nonlinear effects due to temperature and space charge distributions," in *Proc. IEEE Conf. Electr. Insul. Dielectr. Phenomenon (CEIDP)*, Fort Worth, TX, USA, Oct. 2018, pp. 10–13.

[45] Y. Zheng, Y. V. Serdyuk, and S. M. Gubanski, "Space charge controlled electric field preceding inception of electric tree in XLPE at AC voltage," in *Proc. IEEE 11th Int. Conf. Properties Appl. Dielectr. Mater. (ICPADM)*, Sydney, NSW, Australia, Jul. 2015, pp. 132–135.

[46] T. Tanaka, "Charge transfer and tree initiation in polyethylene subjected to AC voltage stress," *IEEE Trans. Electr. Insul.*, vol. 27, no. 3, pp. 424–431, Jun. 1992.

[47] T. Tanaka, "Tree initiation mechanisms," in *Proc. 3rd Int. Conf. Properties Appl. Dielectr. Mater. (ICPADM)*, Tokyo, Japan, Jul. 1991, pp. 18–24.

[48] J. M. Alison, J. V. Champion, S. J. Dodd, and G. C. Stevens, "Dynamic bipolar charge recombination model for electroluminescence in polymer based insulation during electrical tree initiation," *J Phys. D, Appl. Phys.*, vol. 28, no. 8, pp. 1693–1701, Mar. 1993.

[49] Y. X. Zhang, L. Zhang, Y. X. Zhou, M. Chen, and Z. L. Zhou, "DC electrical tree initiation in silicone rubber under temperature gradient," *IEEE Trans. Dielectr. Electr. Insul.*, vol. 25, no. 3, pp. 1142–1150, Jun. 2018.

[50] Y. Sekii, H. Kawanami, M. Saito, K. Sugi, and I. Komatsu, "DC tree and grounded DC tree in XLPE," in *Proc. IEEE Conf. Electr. Insul. Dielectr. Phenomenon (CEIDP)*, Nashville, TN, USA, Oct. 2005, pp. 523–526.

[51] X. Chen, Y. Xu, and X. Cao, "Nonlinear time series analysis of partial discharges in electrical trees of XLPE cable insulation samples," *IEEE Trans. Dielectr. Electr. Insul.*, vol. 21, no. 4, pp. 1455–1461, Aug. 2014.

[52] J. Kindersberger and C. Lederle, "Surface charge decay on insulators in air and sulfurhexafluorid—Part II: Measurements," *IEEE Trans. Dielectr. Electr. Insul.*, vol. 15, no. 4, pp. 949–957, Aug. 2008.

[53] J. G. Simmons and M. C. Tam, "Theory of isothermal currents and the direct determination of trap parameters in semiconductors and insulators containing arbitrary trap distributions," *Phys. Rev. B, Condens. Matter*, vol. 7, no. 8, pp. 3706–3712, Apr. 1973.

[54] Z. L. Li, B. X. Du, Z. R. Yang, and C. L. Han, "Temperature dependent trap level characteristics of graphene/LDPE nanocomposites," *IEEE Trans. Dielectr. Electr. Insul.*, vol. 25, no. 1, pp. 137–144, Jan. 2018.

[55] W. Wang, T. Takada, Y. Tanaka, and S. Li, "Trap-controlled charge decay and quantum chemical analysis of charge transfer and trapping in XLPE," *IEEE Trans. Dielectr. Electr. Insul.*, vol. 24, no. 5, pp. 3144–3153, Oct. 2017.

[56] N. Haque, S. Dalai, B. Chatterjee, and S. Chakravorti, "Studies of the effect of temperature on the charge trapping and de-trapping processes of polymeric insulators through depolarization current measurements," *IEEE Trans. Dielectr. Electr. Insul.*, vol. 24, no. 3, pp. 1896–1904, Jun. 2018.

TAO HAN (M'16) was born in Shandong, China. He received the M.E. and Ph.D. degrees in electrical engineering from Tianjin University, China, in 2012 and 2015, respectively. Since 2015, he has been a Lecturer with the School of Electrical Engineering and Automation, Tianjin University, China. He is currently a Visiting Scholar with the Department of Electrical Engineering, University of Bologna, Bologna. His main research interests include degradation of cable insulation and partial discharge detection.

BOXUE DU (M'00–SM'04) received the M.E. degree in electrical engineering from Ibaraki University and the Ph.D. degree from the Tokyo University of A&T. From 1996 to 2002, he was an Associate Professor with the Niigata Institute of Science and Technology, Japan. From 2000 to 2002, he was a Visiting Scientist with Niigata University, Japan. Since 2002, he has been a Professor and the Director-Founder of the Institute of High Voltage, School of Electrical and Information Engineering, Tianjin University, China. He has published two books and four book chapters in Polymer Dielectrics, and authored about 400 papers and over 100 of them published in the IEEE TRANSACTIONS. His research interests include dielectric failure mechanisms of polymer insulating materials, electrical insulation technology, and application of polymer dielectrics under various extreme environments, such as cryogenic, high temperature, high altitude, gamma-ray irradiation, and high-intensity magnetic field. He is a member of IEEJ, a senior member of CSEE, and a member at several WG in CIGRE. He is an Associate Editor of the IEEE TRANSACTIONS ON DIELECTRICS AND ELECTRICAL INSULATION.

TINGTING MA was born in Hengshui, Hebei, China, in 1992. She received the B.Eng. degree in electrical engineering, in 2017. She is currently pursuing the M.Eng. degree in electrical engineering from Tianjin University. Her research interest includes the growth characteristics of electrical trees in cable insulation material.

FUYU WANG was born in Linfen, Shanxi, China, in 1993. She received the B.Eng. degree in electrical engineering from Datong University, Datong, China, in 2017. She is currently pursuing the M.Eng. degree in electrical engineering with Tianjin University. Her research interest includes aging characteristics of silicone rubber insulation for cable accessories.

YU GAO (M'10) was born in Liaoning, China, in 1981. He received the Ph.D. degree from the School of Electrical and Information Engineering, Tianjin University, Tianjin, China, in 2009. He served as an Associate Professor of high voltage and electrical insulation technology, since 2012. His current research interests include ageing phenomena of polymer insulating materials, pulsed power technology and its application in environment engineering, and over voltage mechanism and protection.

ZHIPENG LEI (M'13) received the B.Sc. degree from East China Jiaotong University, China in 2005, and the M.Sc. and Ph.D. degrees from the Taiyuan University of Technology, China, in 2010 and 2015, respectively. He joined as a Lecturer with the College of Electrical and Power Engineering, Taiyuan University of Technology, since 2015. He is currently a Postdoctorate with the University of Bologna. His main research interests include the condition assessment of high voltage cable failure and associated partial discharges characteristics, and intelligence techniques in coal mine.

CHUANYANG LI was born in Shandong, China, in 1987. He received the double B.S. degrees in electrical engineering and English from the Taiyuan University of Technology, the M.S. degree from the Department of Electrical Engineering, Taiyuan University of Technology, in 2014, and the Ph.D. degree from the Department of Electrical Engineering, Tsinghua University, in 2018. He is currently a Postdoctoral Fellow with the Department of Electrical, Electronic and Information Engineering Guglielmo Marconi of the University of Bologna (Alma Mater Studiorum-Università Di Bologna), Italy. He has authored and coauthored more than 40 scientific papers. His research interests include surface charge behavior, material modification for dielectrics in GIS/GIL, online monitoring for power cable insulation, and PD pattern recognition of HV motors and generators.